3 Structure and Property Characterization of Low-k Dielectric Porous Thin Films Determined by X-Ray Reflectivity and Small-Angle Neutron Scattering

E.K. Lin, H. Lee, B.J. Bauer, H. Wang, J.T. Wetzel, and W. Wu

A methodology to characterize nanoporous thin films based on a novel combination of high-resolution specular X-ray reflectivity and small-angle neutron scattering has been developed. The average pore size, pore connectivity, film thickness, wall or matrix density, coefficient of thermal expansion, and moisture uptake of nanoporous thin films with nonhomogeneous solid matrices can be measured. The measurements can be performed directly on films up to 1.4 μm thick while supported on silicon substrates. Further advancements in the data analysis include the accommodation of additional heterogeneities within the material surrounding nanoscale voids. This method has been successfully applied to a wide range of materials under evaluation as candidates for low-k interlayer dielectrics.

3.1 Introduction

Low-k dielectric materials have been identified by the microelectronics industry as a critical factor to enable deep submicrometer technology for improved performance of integrated circuits. Nanoporous materials have been identified as an important class of low dielectric constant (low-k) materials because the incorporation of voids effectively reduces the dielectric constant of the film [1]. Many strategies have been developed to incorporate pores into thin films, including the thermal decomposition of a porogen within a bulk material, sol-gel processing methods, chemical vapor deposition, and surfactant-templated pore development. Unlike traditional homogeneous dielectric materials, the structure of the porous network affects properties critical to their integration into current fabrication lines. There is a need for the measurement of the on-wafer structural properties of these porous thin films to understand and to predict correlations between processing conditions and the resulting physical properties. Few techniques are able to measure the structural properties of porous films ~1 μm thick supported on silicon substrates. Recently, Gidley et al. [2] use positronium annihilation lifetime spectroscopy to measure void sizes and distributions. Dultsev and Baklanov [3] used ellipsometric porosimetry to also measure void sizes and distributions. Wu et al. [4] have demonstrated that the average void size, porosity, film density, coefficient of thermal expansion, connectivity among voids and moisture uptake can be measured using a combination of high-resolution specular X-ray reflectivity

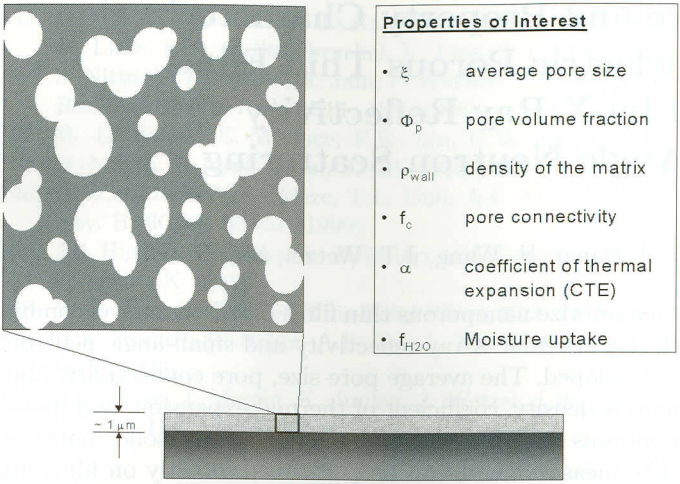

Fig. 3.1. Schematic diagram of the porous thin films of interest in this work. The structural and physical properties measured in this work are listed in the *inset box*

(HRSXR) and (SANS) techniques [5,6]. These measurements are performed directly on films prepared small-angle neutron scattering and supported on silicon substrates. The novelty of this approach to the characterization of porous thin films is two-fold: the use of a new high-resolution X-ray reflectometer to accurately characterize films up to 1.4 μm thick and the use of complementary data obtained from both HRSXR and SANS as a set of simultaneous equations to quantitatively determine structural parameters of porous thin films. These thin-film properties, together with a simple sketch of a thin film, are shown in Fig. 3.1. Results obtained for several classes of porous low-k dielectric thin films have been provided to the semiconductor industry and material suppliers to aid their effort in the selection of candidate materials and processes to be used in next-generation integrated circuits. In this chapter, we first outline the basic methodology, followed by the introduction of a three-phase scheme to enable the characterization of samples with heterogeneities other than nanopores. The intrinsic limitation of this SANS-HRSXR-based methodology will then be discussed and this chapter will end with an outline of the research areas currently under development for further improvements in the accuracy and versatility of this methodology.

3.2 Two-Phase Methodology

In the two-phase method [4] as illustrated in Fig. 3.1, the simplest description of a porous material was used; one phase is comprised of the voids and the other is comprised of the connecting material. The connecting material (the pore-wall material) is assumed to be uniform in composition and in density.

With this assumption, the average density of the film can be parameterized with two unknowns, the porosity, P, and the wall density, ρ_w. These two variables cannot be independently determined from either HRSXR or SANS data. By using both techniques and solving simultaneous equations, specific to each technique and involving these two variables, the values of the unknowns can be determined. In order to perform this analysis, we must also know the chemical composition of the film. The chemical compositions were determined using a combination of Rutherford backscattering (RBS) (for silicon, oxygen, and carbon) and forward-recoil elastic scattering (FRES) (for hydrogen). The film composition is used to convert electron density to mass density in the HRSXR data analysis and to determine the scattering contrast between the connecting material and pores in the SANS analysis. In addition to P and ρ_w, another parameter, the correlation length, ξ, is determined from the SANS data. These three parameters are widely used to characterize two-phase materials. Most of the low-k films analyzed by our group are well characterized using the two-phase model. In this chapter, we illustrate our basic methodology with a representative porous silica thin film.

3.2.1 Experimental

The fundamentals of the three measurement techniques used in this chapter will be discussed briefly at an introductory level. References are provided in each respective section for those interested in more experimental detail.

High-Energy Ion Scattering. The elemental composition of the films is determined by Rutherford backscattering spectroscopy (RBS) for silicon, carbon, and oxygen and forward-recoil elastic spectroscopy (FRES) for hydrogen. In both techniques, a beam of high-energy ions is directed toward the sample surface. The number of scattered particles is counted as a function of their energy [7]. The elemental composition of the film can be determined because the scattered energy is dependent upon the mass of each elemental species. Fits are performed on the scattered peaks to compute the relative fraction of each element. The measurements were performed at the Surface and Thin Film Analysis Facility at the University of Pennsylvania.[1]

X-Ray Reflectivity. High-resolution specular X-ray reflectivity (HRSXR) is a powerful experimental technique to accurately measure the structure of thin films in the direction normal to the film surface. In particular, the film

[1] Certain commercial equipment and materials are identified in this paper in order to specify adequately the experimental procedure. In no case does such identification imply recommendation by the National Institute of Standards and Technology nor does it imply that the material or equipment identified is necessarily the best available for this purpose.

thickness, film quality (roughness and uniformity), and average film density can be determined with a high degree of precision. The coefficient of thermal expansion (CTE) can also be determined from measurements of the film thickness at different temperatures.

High-resolution X-ray reflectivity at the specular condition with identical incident and detector angles, θ was measured using a $\theta/2\theta$ configuration with a fine-focus copper X-ray tube as the radiation source. Typically, the reflected intensity is measured at grazing incidence angles ranging from 0.01° to 2°. The incident beam is conditioned with a four-bounce germanium [220] monochromator.

The beam is further conditioned before the detector with a three-bounce germanium [220] crystal. The resulting beam has a wavelength, λ, of 1.54 Å, a wavelength spread (FWHM), $\delta\lambda/\lambda = 1.3 \times 10^{-4}$, and an angular divergence of 12″. With a goniometer having an angular reproducibility of 0.0001°, this instrument has the precision and resolution necessary to observe interference oscillations in the reflectivity data from films up to 1.4 μm thick.

Given the elemental composition, the average electron density of the porous thin film is easily converted into an average mass density of the film. The average mass density of the film is related to the porosity and wall density of the film through the equation

$$\rho_{\text{eff}} = \rho_{\text{w}}(1 - P)\,, \tag{3.1}$$

where ρ_{w} is the density of the wall material and P is the porosity of the film (by volume). At this point, an assumption of the matrix mass density can provide a numerical estimate of the film porosity. However, no information about the pore size can be obtained using HRSXR.

In addition to the average mass density of the film, the film thickness can be determined from a more detailed analysis of the reflectivity data or the periodicity of the oscillations in the reflectivity profile. For example, the oscillations at larger angles result from the destructive and constructive interference of the X-rays reflected from both the air/film interface and the film/silicon interface. For more detailed structure information, the X-ray reflectivity data are fit using a nonlinear least squares algorithm using the recursive multilayer method [8]. Model profiles are generated and separated in several layers with varying thickness and electron density, and then the resulting reflectivity profiles are calculated. The best fit electron density depth profile to the data provides the overall film thickness, the film roughness, and the average electron density of the film. In this measurement, the electron-density profiles are not necessarily unique fits to the data because phase information is lost.

Small-Angle Neutron Scattering. The small-angle neutron scattering (SANS) measurements are performed on the 8-m NG1 line at the National Institute of Standards and Technology Center for Neutron Research. The

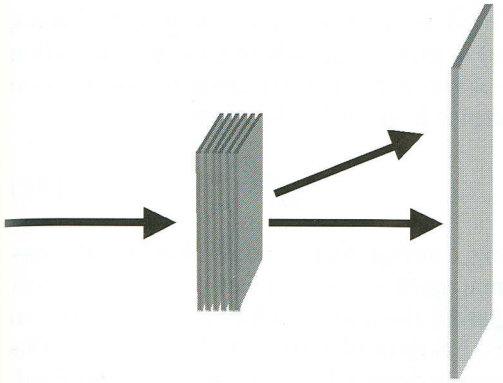

Fig. 3.2. Schematic diagram illustrating the experimental configuration of the small-angle neutron scattering measurement

neutron wavelength, λ, was 6 Å with a wavelength spread $\Delta\lambda/\lambda$ of 0.14. The sample-to-detector distance was 3.6 m and the detector was offset by 3.5° from the incident beam to increase the range of observable angles. The films were placed so that the film surface is perpendicular to the incident beam. The samples are held in either rectangular quartz cells with a 5-mm path length or stainless steel holders with quartz windows and a 4-mm path length. To increase the scattered intensity from these thin films, up to ten sample pieces are stacked within the cell. The single-crystal silicon substrates are essentially transparent to the neutron beam and the scattered intensity arises almost completely from the structure in the porous thin films. Two-dimensional scattering patterns were collected from the sample for up to five hours for sufficient count statistics. The two-dimensional data were then corrected for empty beam and background scattering using standard reduction methods. The scattered intensity was placed on an absolute intensity scale with reference to a water standard. The scattered intensity is presented as a function of q (where $q = 4\pi/\lambda \sin\theta$ and θ is the scattering angle). A schematic diagram of the SANS measurement configuration is shown in Fig. 3.2.

To quantitatively analyze the SANS data, a suitable scattering model must be chosen to describe the data. Thus far, at least four different analysis methods have been used and developed to analyze SANS data from porous thin film samples, a simple two-phase Debye model [9], a three-phase Debye model [10], and the Porod model and scattering invariant calculation. In the following, the two-phase Debye model, the simplest and the most commonly used, is used to illustrate this technique.

3.2.2 Two-Phase Analysis Using the Debye Model

The two-phase model is the simplest model to describe a high-porosity material. In this model, there are only two phases, the pores and the matrix material. Additionally, the matrix material is assumed to be homogenous. Debye developed the formalism describing the scattering that arises from

a random two-phase structure. The density correlation function describing the structure is assumed to be $\gamma(r) = \exp(-r/\xi)$, where ξ is the correlation length. The average chord length of the pores is then given by the relation $I_c = \xi/(1-P)$ and the SANS intensity is given by the equation

$$I(q) = \frac{8\pi P(1-P)\Delta\rho_n^2\xi^3}{(1+q^2\xi^2)^2}\,, \tag{3.2}$$

where $\Delta\rho_n$ is the neutron-scattering contrast and is determined by the elemental composition of the solid matrix material and is linearly dependent upon ρ_w. The correlation length, ξ, and the scattered intensity at $q = 0$, can be determined by linearly fitting SANS data plotted as $1/I^{1/2}$ vs. q. At this point in the analysis, only the correlation length is quantitatively determined.

To determine the film porosity, P, and the matrix mass density, we must use additional information from SXR. Given $I(0)$ and ξ, (3.2) becomes a function only of ρ_w and P. From the SXR formalism, (3.1) is also a function of ρ_w and P. With two equations and two unknowns, ρ_w and P, we can solve for these two quantities for the porous thin film. The two-phase model often provides reasonable values for the density of the wall material, but these values arise after assuming that the connecting material is homogeneous. Inhomogeneities in the connecting material could lead to changes in the scattered intensity.

The pore connectivity and moisture uptake of the film can also be determined using the Debye formalism. The samples are placed into quartz cells and immersed in either deuterated toluene (d-toluene) or deuterated water (D_2O). The d-toluene solvent is chosen because it readily wets the samples studied by us thus far. If either of the deuterated solvents penetrates open and interconnected pores, the absolute value of the scattered intensity changes because of the large contrast change in $\Delta\rho_n^2$ from air or vacuum in the pores to a deuterated material. If all the pores within a sample were filled with d-toluene, the entire scattered intensity would increase by a factor of $\sim$20 depending on the composition and wall density. If the increase in scattered intensity is less than the predicted value, then only a fraction of the pores are filled with the solvent. In a similar manner, the moisture uptake of D_2O may also be determined. In this methodology, pore connectivity represents the fraction of pores that are interconnected and accessible to a solvent at the outside surface.

3.2.3 Results and Discussion

As an example, we present data and results from a porous silica thin film prepared from a methyl silsesquioxane (MSQ) spin-on glass resin processed with a porogen material. The porogen material forms domains in the film that are subsequently burned off to form a porous structure. The elemental composition of the film (molar per cent) was determined to be 20% silicon,

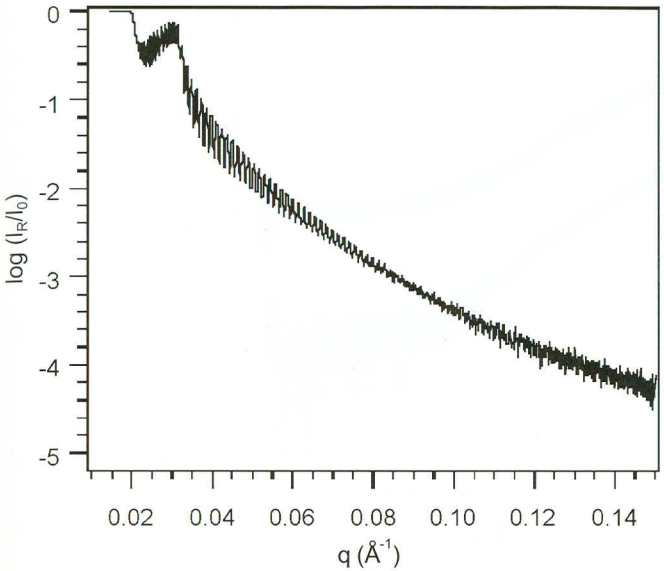

Fig. 3.3. X-ray reflectivity data showing the logarithm of the reflected intensity as a function of q

35% oxygen, 14% carbon, and 31% hydrogen. The standard uncertainty associated with the molar fraction of each element is ±5% (10). The elemental composition of the film is needed to calculate the contrast factors in both the X-ray reflectivity and SANS equations and allows for a quantitative determination of the film porosity and matrix wall density.

In Fig. 3.3, the X-ray reflectivity profile of the film is plotted as the logarithm of the reflectivity (I_R/I_0) as a function of q, where $q = (4\pi/\lambda)\sin\theta$. At low q values, the reflectivity is unity and the X-ray beam is almost totally reflected from the sample surface. At a critical value of q, the reflectivity drops sharply as the X-ray beam begins to penetrate the film. The angular value of the critical angle provides a measure of the average electron density of the film. Given the elemental composition of the film, the average mass density of the film, including the pores, can be determined in a straightforward manner [4]. The average electron density from the critical angle of this film was determined to be (0.289±0.005) electrons/Å^3 and the average mass density was (0.94±0.01) g/cm^3. All the uncertainties reported in this work are their 1σ values. At slightly higher q values, a second critical angle is evident and represents the critical angle of the silicon substrate. The numerous oscillations in the reflectivity profile are due to the constructive and destructive interference from X-rays reflected from the film/air interface and the film/silicon interface. The periodicity of the oscillations provides a very precise measurement of the thickness of the film. The thickness of this film was determined to be (4240±10) Å. The coefficient of thermal expansion

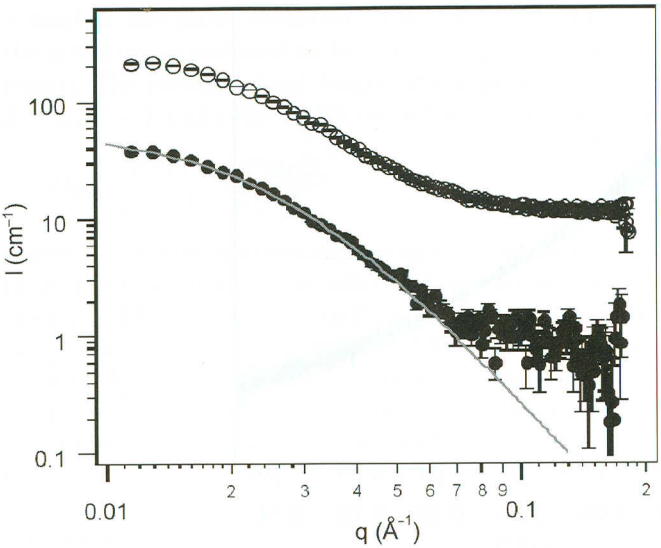

Fig. 3.4. Small-angle neutron scattering data for a stack of films under ambient conditions (*filled symbols*) and immersed in deuterated toluene (*open symbols*). The *solid line* is the best fit to the data using the Debye model [9]

of the film could be determined by measuring the thickness of the film at different temperatures, but is not presented here.

In Fig. 3.4, the SANS data for both the film in the ambient atmosphere (air) and immersed in deuterated toluene are shown on an absolute intensity scale as a function of the magnitude of the scattering vector q. Also shown is the best fit to the data for the film in air using the Debye formula. The Debye equation fits the SANS data very well, strongly suggesting that the pore structure has a random two-phase structure. Some porous structures cannot be fit with the Debye equation and other analysis methods for the SANS data are required [5,6]. The data at higher q values for both sets of SANS data are relatively constant and result from the incoherent background scattering from hydrogen (for the sample in air) and the solvent (for the sample in deuterated toluene).

From the Debye model fits to the data, the average pore size of the film can be determined from the size of the correlation length in the Debye model. This quantity is not directly the average pore size, but is related to the average pore size once the film porosity is determined. The correlation length of this film is (37±1) Å. The scattering intensity is also significantly stronger for the film immersed in *d*-toluene than for the film in air. The increase in the intensity is due to the enhanced scattering contrast from a deuterated solvent that has penetrated the film. The fraction of pores that are connected and accessible to the film surface can be determined from the magnitude of the increase in scattering intensity. For this film, the volume fraction of

connected pores is determined to be (56±2)%. Lastly, the film porosity and matrix material density can be determined by combining data from all three experimental techniques because equations from both X-ray reflectivity and SANS are functions of porosity and matrix material density. The parameters are calculated by solving two equations for the two variables of interest (3.4–3.6). For the film in this chapter, the porosity was determined to be (0.26±0.05) and the matrix wall density was (1.26±0.05) g/cm^3. Given the porosity, the average chord length or the average pore size is (50±1) Å.

3.3 Three-Phase Methodology

The two-phase methodology has been successfully applied for many materials from different sources. However, some samples exhibit SANS intensities higher than could be accounted for from a two-phase material given its measured elemental composition. The high SANS intensity reflects the existence of heterogeneities other than from the nanopores within the sample. To force a fit to the SANS data using the two-phase model results in unrealistically high values for the density of the material surrounding the voids. To ensure more reasonable values, an additional phase was introduced within the matrix material, i.e. of the presence of three phases was assumed in modeling the thin-film structure. The underlying principles for both the three-phase and the two-phase methodology are identical; both rely on the complementary nature of the results from SANS and HRSXR. The difference lies in the model used to interpret the SANS results. Consequently, the results on CTE, film thickness, and the electron density are unchanged with regard to the specific methodology used because these quantities are determined solely from HRSXR data.

In this section, the theoretical development of the three-phase model will be outlined and then followed by an example to illustrate its application. For a two-phase system, the neutron scattering contrast, η^2, can be expressed as

$$\eta^2 \propto P(1-P)\left(\rho_{\mathrm{w}} \sum (n_i b_i / m_i)\right)^2 , \tag{3.3}$$

where P again is the porosity or the volume fraction of the voids, and b_i, n_i and m_i denote the neutron scattering length, the number fraction and the atomic weight of element i, respectively. Equation (3.3) sums over all the elements in the samples. The observed SANS intensity dictates the magnitude of η^2 and the HRSXR data determine the value of the product $\rho_{\mathrm{w}}(1-P)$. In samples with significant amounts of hydrogen, the observed SANS intensity (and hence η^2) can only be accounted for with an unrealistic value of ρ_{w}. For example, a sample with the following composition by number, Si (16%), O (26%), C (19%) and H (39%) was measured and HRSXR results indicated that the film density was (0.72±0.01) g/cm^3. Using a combination of SANS and HRSXR data, the calculated value of ρ_{w} was (3.30±0.2) g/cm^3, a value

higher than that of quartz and unrealistic. The corresponding porosity was (78±1.5)%. Samples with significant hydrogen content are among those likely to fail using the two-phase model. In neutron scattering, the hydrogen atom is rather unique in terms of its scattering length, b_{H}, of -0.374 ($\times 10^{-12}$ cm). While the neutron scattering lengths of silicon, oxygen, and carbon have positive values, minor deviations in the spatial distribution of hydrogen are expected to cause a major enhancement in SANS intensity. In our interpretation, unrealistically high wall density values result from an inhomogeneous distribution of hydrogen atoms within the wall or matrix material.

The three-phase model is developed as a simple approximation to account for the heterogeneous distribution of constituent elements within the film. The hydrogen content was chosen to be the focal point of this SANS model because of its negative neutron scattering length. We further assume that all the hydrogen and carbon atoms exist as hydrocarbons and are segregated from the silicon and oxygen atoms because it is unphysical to have all the hydrogen atoms forming independent phases or clusters. The nanoporous thin film is then assumed to be comprised of the following three phases, the hydrocarbon phase (phase 1), the silicon and oxygen or silica phase (phase 2) and the voids (phase 3). The corresponding contrast factor of a three phase-material can be expressed as

$$\begin{aligned}\eta^2 \propto\ & \Phi_1(1-\Phi_1)(B_2-B_1)(B_3-B_1)\\ & +\Phi_2(1-\Phi_2)(B_3-B_2)(B_1-B_2)\\ & +\Phi_3(1-\Phi_3)(B_1-B_3)(B_2-B_3)\,,\end{aligned} \tag{3.4}$$

where Φ_j stands for the volume fraction occupied by phase j [10]. By definition, Φ_3 is equal to P, the porosity of the film. B_j is the neutron scattering length of phase j and is defined as $\rho_j \sum(n_i b_i/w_i)$ where ρ_j is the mass density of phase j and the summation is over all the elements existed in phase j. Also by definition, B_3, the neutron scattering length of voids, is zero. Within the above equation there are a total of five unknowns, Φ_1, Φ_2, Φ_3, ρ_1, and ρ_1. There are two obvious constraints or relations for these unknowns and they are;

$$\sum \Phi_i = 1\,, \tag{3.5}$$

for the sum of all three volume fractions to be unity, and

$$\Phi_1\rho_1/\Phi_2\rho_2 = (n_{\mathrm{c}}m_{\mathrm{c}} + n_{\mathrm{H}}m_{\mathrm{H}})/(n_{\mathrm{Si}}m_{\mathrm{Si}} + n_{\mathrm{O}}m_{\mathrm{O}})\,, \tag{3.6}$$

where the mass ratio between phases 1 and 2 is equal to the ratio of the total mass of the constituents. At this point, there are still three unknowns. The HRSXR data provide an additional relation or constraint for these unknowns. More explicitly,

$$Q_{\mathrm{c}}^2 \propto (\Phi_1\rho_1 + \Phi_2\rho_2)/(\Phi_1 + \Phi_2)\,, \tag{3.7}$$

where Q_c^2 is proportional to the critical angle expressed in Fourier space as measured by HRSXR, and the right-hand side of the above equation is, by definition, the matrix material or the wall density. The SANS data provide a measure of η^2 of (3.4), but one more experimental measurement of some of the five variables is needed. In this chapter, we assume that the density of hydrocarbon phase, ρ_1, is 1.0 g/cm^3. This is a reasonable assumption because the bulk density of many hydrocarbons is close to g/cm^3.

The sample mentioned above was reanalyzed using the three-phase model and the matrix density was found to be (1.71±0.05) g/cm^3, a value close to that of a thermally grown silicon oxide and its porosity was (58±1.5) %. This example does not necessarily prove that the matrix material surrounding the voids is indeed made of two phases, a hydrocarbon phase and a silica phase. However, this result is consistent with the notion that the matrix is not a homogeneous one-phase material. The three-phase model discussed here is the simplest extension of the two-phase model and its application is limited to cases where the two-phase methodology fails to provide physically meaningful results. The two-phase and three-phase models, however, provide bounding limits on the average density of the matrix material.

In addition to all six ρ_i and Φ_i parameters, three correlation lengths, ξ_i, one for each phase i, are needed to fully characterize a three-phase system. It is noteworthy that there is only one correlation length for a two-phase system and its value can be deduced directly from the SANS data using Debye, Porod, or other analysis schemes [10]. For a three-phase system, all three correlation lengths manifest themselves in the SANS results via a relation similar to that of (3.4). Each correlation length is weighted by the neutron scattering contrast factor of that particular phase. Conveniently, the neutron contrast factor of hydrocarbons, especially for those with a 1:2 carbon to hydrogen ratio, is nearly zero because the scattering length of hydrogen is -3.74×10^{-13} cm and 6.65×10^{-13} cm for carbon. Accordingly, the measured correlation length from SANS is dominated by that of the phase composed of silicon and oxygen. The correlation length in our example can be treated as if the system is a two-phase system with a silicon-oxygen phase and a voids-hydrocarbon phase. The chord length of each phase can be deduced with the two-phase scheme [10].

After the structural parameters are determined with the three-phase model, the pore connectivity and moisture uptake can be determined using the methodology developed for the two-phase system. The pore connectivity and moisture uptake were measured by conducting SANS measurement on samples immersed respectively in a deuterated organic solvent and in deuterated water. Organic solvents with low interfacial tension can readily fill interconnected pores having a passage to the exterior surface to cause a scattering contrast change. Deuterated toluene has been used for all of the samples tested because it spreads readily on surfaces of those samples. Once the pores are filled, the scattering contrast changes dramatically depending on the neu-

tron scattering length of the solvent used. The percentage of the pores filled by solvent or water can be determined from the difference in SANS intensities between thin films before and after immersion.

3.4 Films with Ordered Porous Structure

The Debye analysis of the SANS data assumes a random two-phase structure with an exponential correlation function. This description and related analysis are found to be appropriate for a large class of samples. Another class of samples possesses a highly ordered porous structure, as evidenced by the pronounced scattering peaks in Fig. 3.5. A modified data-analysis procedure is needed to treat the SANS data.

The invariant analysis scheme chosen here to analyze ordered samples is analogous to earlier analysis methods for polycrystalline samples, within which ordered domains are randomly oriented and packed throughout the film. The scattering invariant, Q, was calculated by using

$$\text{Invariant} = 4\pi \int_0^\infty q^2 I(q) dq \,. \tag{3.8}$$

However, if the c-axis of the ordered domains is parallel to the substrate [11,12], the invariant calculation must be modified by dividing the scattering intensities into contributions from the background part and the discrete peaks. In this case, the invariant is calculated as a sum of two terms. The background part of the intensity is attributed to the randomly oriented do-

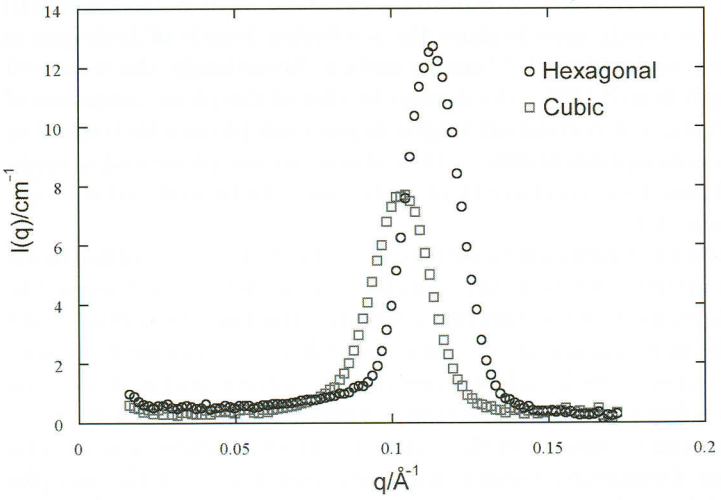

Fig. 3.5. SANS intensities from two nanoporous films with obvious ordered porous structure

mains and its invariant is calculated using the same equation as above. The invariant of the discrete peak can be approximated by

$$\text{Invariant} = 2\pi q_{\text{Max}}(\pi \Delta q^2/4) I_{\text{Max}} \,, \tag{3.9}$$

where q_{Max} is the peak position, I_{Max} the peak height, and Δq the peak full width at half intensity. The invariant is related to the porosity in a similar functional form from the Debye analysis, i.e. $8\pi^3 \Delta\rho^2 \Phi(1-\Phi)$. The calculated value of invariant is related to both ρ_{w} and P; this result combined with the data from HRSXR again enables the values of P and ρ_{w} to be determined.

SANS measurements with samples positioned at an oblique angle were also conducted to verify the notion that the c-axis of the ordered domain was parallel to the thin-film surface. On a two-dimensional detector the result given in Fig. 3.5 appeared as a high-intensity ring centered around the beam stop when the incident beam was perpendicular to the film changed quickly into two high-intensity spots once the sample was rotated with the maximum located along the rotation axis. If the domain structure within the films was randomly oriented, rotation of the sample with respect to the incident beam was not expected to result in a change from a maximum ring to two spots. It is essential to perform the abovementioned experiment before using (3.9) for the invariant calculation.

3.5 Limits of SANS Characterization Methods

Most of the ILD candidates from industry provide enough SANS signal for quantitative data treatment, following either a two-phase or three-phase scheme. However, the SANS intensity from some samples was just barely within above the detection limit of the SANS instrumentation. However, the results from composition analysis and HRSXR of these samples suggest that a significant porosity exists. The low SANS intensity is simply due to a small correlation length, ξ, or pore size. Based on (3.2), the SANS intensity is proportional to ξ^3 for any fixed porosity. The correlation length, ξ, is determined by the angular dependence of the scattered intensity. As the pore size becomes small, the SANS intensity becomes weak and flat. At some point, the scattering is not sufficient to produce a reliable signal above the detector noise level. The scattered intensity also becomes a weaker function of the scattering parameter q, so that the instrumentally accessible range of q also limits the minimum size that can be measured. At this point, the distinction between a dense matrix with very small pores and a homogeneous low-density matrix is lost. The exact limits of the SANS technique depend on sample characteristics and instrumental factors. In general, SANS measurements become unreliable as the correlation lengths fall below 5 Å.

As an example of the scattering limits, consider two samples with identical porosity but different porous structure, one having uniform 100 Å pores

and the other with a 50/50 mix of 5 Å and 100 Å pores. Their SANS intensities in the low-q region are expected to have an identical shape and fits of the data in that range would both give correlation lengths of approximately 100 Å because the scattering is dominated by the large pores. The zero-angle scattering would be almost cut in half for the sample with bimodal distribution. Applying the two-phase methodology outlined in this chapter, the resultant wall density of the bimodal sample will be the average of the solid wall density and the 5 Å pores.

3.6 Future Developments

3.6.1 Contrast Variation SXR

In order to extend the applicability of the HRSXR-SANS-based methodology to films with pore size in the range of 1 nm or less, we propose a new methodology based on HRSXR alone. In essence, what we propose is analogous to the ellipsometry porosimetry method developed recently by Dultsev and Baklanov [3] where the refractive index and the thickness of thin films are determined by ellipsometry at different vapor pressures of an absorbate. The pore-size distribution is then derived using the Kelvin equation. In the present case, HRSXR is used in lieu of ellipsometry. The main advantage of using HRSXR is that the depth dependence of the porosity can be obtained. To illustrate the feasibility of this method, in situ X-ray reflectivity measurements were conducted in saturated toluene vapor at room temperature on three samples. Each of these samples was found to have relatively low SANS intensity due to small pore size. Films that have been measured in air by HRSXR in the conventional way are then soaked in toluene for several hours. The wet samples were placed in the HRSXR apparatus along with a container of solvent to saturate the atmosphere and inhibit evaporation from the pores of the film. The results for both the dry and toluene-soaked films of samples 26, 27, and 28 are shown in Fig. 3.6. The curves are shifted in pairs for clarification. All three samples have shifts in their critical edge to higher q indicating a higher electron density due to toluene replacing some or all of the air in the film voids. Sample 27 also retains the fringes, allowing for calculation of the film thickness. Sample 26 loses the fringes probably due to a roughening of the film, while sample 28 seems to have a rough surface with and without the toluene present. We focus the rest of the discussion on sample 27.

The thickness of sample 27 does not change significantly upon swelling, going from 6550 Å to 6890 Å. The total mass density of the film from the critical edge goes from 0.94 g/cm^3 to 1.34 g/cm^3. Once the X-ray results at different toluene vapor pressures become available, the pore-size distribution of these films can be deduced just as in the case of ellipsometry porosimetry. However, even without the full data as a function of vapor pressure, one can still proceed to determine the porosity and the averaged pore size by combining

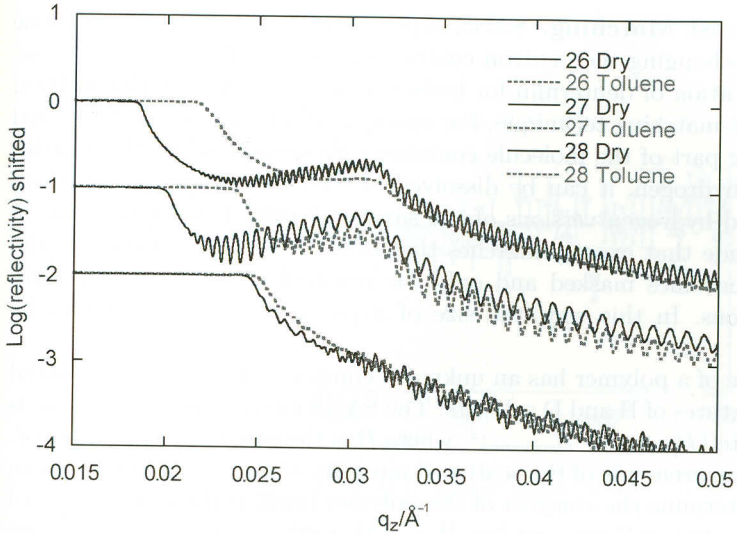

Fig. 3.6. X-ray reflectivity results from three films with relative low SANS intensity. Results from both dry and toluene-soaked samples are shown

the X-ray results from both ambient and vapor-saturated samples. Assuming that all of the pores have become filled with toluene under saturated toluene vapor, the calculated porosity of the film is 0.46, the wall density is 1.74, and the pore size is 5.3 Å. This pore size comes from a combination of HRSXR in air and toluene and the assumption of an exponential correlation function for the SANS data. With the assumption that all the pores are accessible to toluene, pore sizes can be determined by HRSXR alone. This approach is suggested as an alternative when the pore size becomes very difficult to measure by SANS.

3.6.2 Inhomogeneous Wall Composition

In a previous section we introduced a three-phase model to approximate the structure of porous films with heterogeneous matrix. More specifically, the calculation was based upon the assumption of the existence of hydrocarbon-rich (H and C atoms) regions and silica-rich (Si and O atoms) regions. The heterogeneity gives rise to additional scattering intensities in comparison with porous film with a uniform matrix. If the two-phase equation is applied to a sample with a three-phase morphology, the calculated wall density will be higher than the actual average wall density. A single scattering experiment is not expected to distinguish between these two cases, and a more complex set of experiments will be necessary. Here, we propose an alternative SANS experimental methodology to unambiguously determine the phase structure or the homogeneity of the matrix material.

SANS Contrast Matching. SANS experiments are very flexible because of the ease of changing the neutron contrast of a material of interest via selective substitution of deuterium for hydrogen. One example of this method is the contrast-matching technique. For example, if a molecule is synthesized with a specific part of the molecule containing deuterium, while the remainder contains hydrogen, it can be dissolved in solvents that are mixtures of deuterium and hydrogen versions of the same molecule. If a combination of solvents is made that exactly matches that of the deuterium portion of the molecule, it becomes masked and only the remainder of the molecule will scatter neutrons. In this way, the size of a portion of a molecule can be measured.

If a sample of a polymer has an unknown composition, it can be dissolved in various mixtures of H and D solvents. The SANS intensity of each sample is proportional to $(B_{\text{polymer}} - B_{\text{solvent}})^2$, where B is the neutron contrast factor. Therefore, measurements of the scattered intensity of a series of mixtures can be used to determine the contrast of the polymer itself. If the composition of the polymer is not uniform, but has H and D portions, then a match point cannot be achieved, with matching of each component being possible, but simultaneous matching of both not possible. For such a sample, it may be possible to identify the compositions of each of the individual parts.

This technique could be used for the characterization of porous thin films. If the pores are completely accessible from the outer surface with homogeneous walls structure, the wall density can be found. If the pores are completely connected, but the wall is heterogeneous, the average wall density could be found with information on the extent of heterogeneity also being possible. If there are closed pores present, the contrast-match experiment will give a density value of the average of the wall and the closed pores. Another advantage is that this technique is not dependent on the distribution of pore sizes. For (3.1) to be valid, an exponential pore-size distribution is necessary. While this is often the case, samples such as these two shown in Fig. 3.5, which have a peak in the SANS due to an ordered structure, cannot be analyzed in this way. The contrast-match approach can still find a wall density, however.

The contrast-match approach can be demonstrated with some existing data. Many samples have SANS data for both starting sample (air) and solvent immersed (toluene). If the pores are interconnected and are completely wetted by the solvent, then the match point of the average density can be calculated from

$$\rho_{\text{W}} = \frac{\rho_{\text{T}}\sigma_{\text{T}}}{\sigma_{\text{W}}} \left(\frac{(I_{\text{A}}(q))^{1/2}}{(I_{\text{A}}(q))^{1/2} + (I_{\text{T}}(q))^{1/2}} \right) , \tag{3.10}$$

where A is air, T is toluene, and W is wall. For each $I(q)$, (3.10) can be used to calculate an average SANS density where the scattering would go to zero. If the atomic composition is known, then the mass density can be calculated.

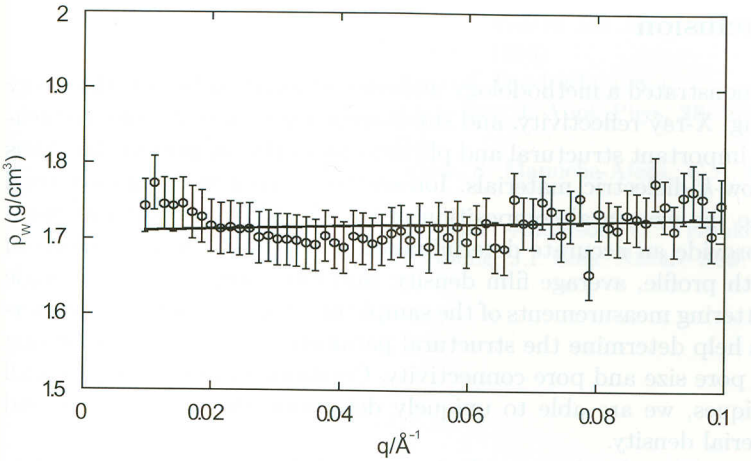

Fig. 3.7. Calculated density of an ILD sample using (3.10)

Several samples that are reported to have open pores were analyzed in this manner. Since the incoherent baseline was not available, it was approximated by a Iq^4 vs. q^4 plot and the slope in the region $0.0001\ \text{Å}^{-4} < q^4 < 0.0005\ \text{Å}^{-4}$ was taken as the baseline and subtracted from the raw data. Equation (3.10) was applied at q values between 0.02 and 0.08 Å^{-1} to calculate ρ_w.

The above figure is a plot of the calculated densities of an earlier version of Nanoglass sample. The density calculated is 1.70 g/cm^3 as compared to 1.63 g/cm^3 calculated from the Debye method, but are all within a reasonable range for a single-phase material of this type. Some uncertainties in the contrast-match measurements are correlated and will cancel. For example, errors in absolute intensity calibration or thickness will be present for both the air and toluene samples and not affect the calculated densities.

Another possible variation on the technique would be to use a supercritical gas, such as CO_2, as the "solvent" in the pressurized scattering cell. By controlling the pressure, one can continuously vary the contrast factor for a single sample. Also, since the gas will be supercritical, wetting will not be a problem and changing the morphology through capillary action will not be a problem. The present Polymers Division or NCNR cells can easily go to 1000 atm and one in construction now will go to 4000 atm. Also, the incoherent scattering baseline that is present in common hydrogen-containing solvents, is insignificant compared with CO_2, so that data analysis near the match point is practical. The Polymers Division pressure cell and controller being modified to accommodate the samples and the CO_2, and model samples will be tested in the near future.

3.7 Conclusion

We have demonstrated a methodology utilizing information from high-energy ion scattering, X-ray reflectivity, and small-angle neutron scattering to measure several important structural and physical properties of porous thin films for use as low-k dielectric materials. Ion-scattering measurements are used to determine the elemental composition of the film. X-ray reflectivity measurements provide an accurate determination of the film thickness, electron density depth profile, average film density, and film roughness. Small-angle neutron scattering measurements of the sample in air and immersed in deuterated liquids help determine the structural parameters of the pores including the average pore size and pore connectivity. Combining information from all three techniques, we are able to uniquely determine the film porosity and matrix material density.

This methodology has been applied to several classes of porous thin films including samples with highly ordered nanopores and samples with additional heterogeneity within the matrix. The limitation of this methodology, primarily originated from SANS measurements, was also discussed together with a plan for future improvements. Additional experimental and theoretical developments are underway to improve the precision in the measurement of the matrix material density and determine structural parameters from heterogeneous thin films.

Acknowledgement. The authors would like to thank Professor Russ Composto of the University of Pennsylvania for his assistance in the high-energy ion scattering experiments.

References

1. L.W. Hrubesh, L.E. Keene, V.R. Latorre: J. Mater. Res. **8**, 1736 (1993)
2. D.W. Gidley, W.E. Frieze, T.L. Dull, A.F. Yee, C.V. Nguyen, D.Y. Yoon: Appl. Phys. Lett. **76**, 1282 (2000)
3. F.N. Dultsev, M.H. Baklanov: Electron. Solid State Lett. **2**, 192 (1999)
4. W.L. Wu, W.E. Wallace, E.K. Lin, G.W. Lynn, C.J. Glinka, E.T. Ryan, H.M. Ho: J. Appl. Phys. **87**, 1193 (2000)
5. E.K. Lin, W.L. Wu, C. Jin, J.T. Wetzel: "Structure and Property Characterization of Porous Low-k Dielectric Constant Thin Films Using X-ray Reflectivity and Small-angle Neutron Scattering", in *Materials, Technology, and Reliability for Advanced Interconnects and Low-k Dielectrics*, ed. by K. Maex et al., MRS Proceedings **612**, D5.22.2 (2001)
6. W.L. Wu, E.K. Lin, C. Jin, J.T. Wetzel: "A Three-Phase Model for the Structure of Porous Thin Films Determined by X-ray Reflectivity and Small-Angle Neutron Scattering", in *Materials, Technology, and Reliability for Advanced Interconnects and Low-k Dielectrics*, ed. by K. Maex et al., MRS Proceedings **612**, D4.1.1 (2001)

7. J.R. Tesmer, M. Nastasi: *Handbook of Modern Ion Beam Materials Analysis* (Materials Research Society, Pittsburgh 1995)
8. J. Lekner: *Theory of Reflection* (Nijhoff, Dordrecht 1987)
9. P. Debye, H.R. Anderson, H. Brumberger: J. Appl. Phys. **28**, 679 (1957)
10. W.L. Wu: Polymer **23**, 1907 (1982)
11. H. Yang, A. Kuperman, N. Coombs, S. Mamiche-Afara, G.A. Ozin: Nature **379**, 703 (1996)
12. Y. Lu, R. Ganguli, C.A. Drewien, M.T. Anderson, C.J. Brinker, W. Gong, Y. Guo, H. Soyez, B. Dunn, M.H. Huang, J.I. Zink: Nature **389**, 364 (1997)